

Original Article

AGAP2-AS1/BRD7/c-Myc signaling axis promotes skin cutaneous melanoma progression

Lei Wu^{1*}, Shenyi Li^{2*}, Jinfu Xu³, Cong Shen^{3,4}, Qihong Qian¹

¹Department of Dermatology, First Affiliated Hospital of Soochow University, Suzhou 215006, Jiangsu, China;

²Department of Obstetrics and Gynecology, Affiliated Hospital of Jiangnan University, Wuxi 214062, Jiangsu, China; ³State Key Laboratory of Reproductive Medicine, Department of Histology and Embryology, Nanjing Medical University, Nanjing 211166, Jiangsu, China; ⁴State Key Laboratory of Reproductive Medicine, Center for Reproduction and Genetics, Suzhou Municipal Hospital, The Affiliated Suzhou Hospital of Nanjing Medical University, Gusu School, Nanjing Medical University, Suzhou 215002, Jiangsu, China. *Equal contributors.

Received October 31, 2022; Accepted December 19, 2022; Epub January 15, 2023; Published January 30, 2023

Abstract: Objective: To examine the effects and mechanisms of AGAP2 Antisense RNA 1 (AGAP2-AS1) in progression of skin cutaneous melanoma (SKCM). Methods: AGAP2-AS1 expression and SKCM survival outcomes were assessed using bioinformatics analysis. In vitro and in vivo assays, including cell proliferation, colony formation, migration, and tumor formation assays, were performed to detect AGAP2-AS1 oncogenic effects in SKCM. RNA pull-down, RNA immunoprecipitation (RIP), and co-immunoprecipitation were used to evaluate the mechanism of AGAP2-AS1 in SKCM progression. Results: AGAP2-AS1 was upregulated in human SKCM tissues and cells and predicted a worse prognosis. AGAP2-AS1 silencing in two SKCM cell lines inhibited cell proliferation, as well as colony formation and migration both in vitro and in vivo. The RNA pull-down assay and RIP analysis results indicated that AGAP2-AS1 interacted with bromodomain containing 7 (BRD7). AGAP2-AS1 knockdown attenuated the BRD7 and c-Myc interaction, which reduced c-Myc expression. The altered phenotypes found in AGAP2-AS1- and BRD7-deficient cells were rescued by overexpression of c-Myc. Conclusions: AGAP2-AS1 participated in oncogenesis in SKCM via the BRD7/c-Myc signaling pathway. These results suggest a molecular mechanism for AGAP2-AS1 in the carcinogenesis of SKCM.

Keywords: AGAP2-AS1, skin cutaneous melanoma, BRD7, c-Myc

Introduction

About 5% of all cases of skin cancer and > 75% of skin cancer-related deaths are associated with skin cutaneous melanoma (SKCM) [1]. With the application of targeted therapies and immunotherapies, patients with SKCM with localized or regional disease have 5-year survival rates of 98% and 64%, respectively [2]. However, SKCM has a high potential for recurrence, intrinsic or acquired resistance, and brain metastasis [3]. The 5-year survival rate of patients with metastatic SKCM is 23% [2]. The mechanisms associated with these outcomes are not fully clarified. Therefore, identifying novel SKCM molecular markers and new effective therapeutic strategies is critical.

Long non-coding RNAs (lncRNAs) with abnormal functions have been implicated in the pathogenesis of diverse human diseases, par-

ticularly in multiple types of cancers, including SKCM [4]. lncRNAs have an oncogenic role in gene regulation because they are sponges for microRNAs [5, 6], decoys for regulatory proteins [7], and scaffolds for protein-protein interactions [8]. These characteristics affect components of tumor progression, including invasion, metastasis, inter- and intra-tumor heterogeneity, therapy resistance, and cell proliferation [9, 10]. More investigations of tumor-associated lncRNA effects and underlying mechanisms are needed to reveal molecular biological changes that drive SKCM progression.

AGAP2 Antisense RNA 1 (AGAP2-AS1) is a novel oncogenic lncRNA that is involved in cancer tumorigenesis and progression, including glioblastoma and colorectal, breast, gastric, esophageal, and non-small-cell lung cancer [11-19]. It is also strongly associated with a poor prognosis. AGAP2-AS1 acts as a scaffold and interacts

AGAP2-AS1 promotes skin cutaneous melanoma progression

directly with EZH2 (enhancer of zeste homolog 2) and LSD1 (lysine-specific demethylase 1A) to form a signaling network to affect the function of multiple target genes (e.g., *TFPI2*, *LATS2*, and *KLF2*) [13, 19]. AGAP2-AS1 may also participate in cell proliferation, migration, and invasion, but it is not clear whether AGAP2-AS1 and other oncogenes co-regulate SKCM development.

In this study, we examined the carcinogenic effects and associated underlying mechanisms of AGAP2-AS1 in SKCM. We analyzed data from the Cancer Genome Atlas (TCGA) to examine the expression and prognostic value of AGAP2-AS1 in SKCM. We investigated the effects of AGAP2-AS1 on cancer cell proliferation, colony formation, and migration in vitro and in vivo. We also investigated the role of bromodomain containing 7 (BRD7), a potential candidate AGAP2-AS1 target protein, during tumorigenesis using RNA immunoprecipitation (RIP) and RNA pull-down assays. Finally, we investigated the potential mechanism of AGAP2-AS1 and the BRD7/c-Myc signaling pathway in SKCM progression.

Materials and methods

Bioinformatics analysis

AGAP2-AS1 expression levels in SKCM samples and normal tissues were obtained from the Genotype-Tissue Expression database (<https://gtexportal.org/>) and TCGA (<https://portal.gdc.cancer.gov/>). An analysis of the correlation of AGAP2-AS1 with tumor pathological stage was performed using data from the TCGA. Based on the median level of AGAP2-AS1 expression, cases were designated as high or low AGAP2-AS1. Kaplan-Meier survival curve analysis was used to analyze relationships between AGAP2-AS1 expression levels and SKCM survival outcomes, including disease-specific survival, disease-free interval, and overall survival (OS).

Fluorescence in situ hybridization

Fluorescence in situ hybridization (FISH) kits (RiboBio, Guangzhou, China) were used to perform FISH analysis following the protocol of the manufacturer. SKCM tissue microarrays were deparaffinized and permeabilized for 5 min. Sections were then incubated with pre-hybridization buffer for 30 min. FISH probes were mixed with pre-warmed hybridization buffer,

added to the sections, and incubated overnight (37°C, in the dark); 4',6-diamidino-2-phenylindole was used to counterstain cell nuclei. The results were analyzed using confocal fluorescence microscopy (LSM800; Zeiss, Oberkochen, Germany).

RNA extraction and quantitative real-time polymerase chain reaction (qRT-PCR)

TRIzol reagent (Invitrogen, Carlsbad, CA, USA) was used to extract total RNA from tissues and cultured cells. Then, reverse transcription and PrimeScript RT reagent (Takara Bio, Kusatsu, Japan) were used to synthesize complementary DNA from total RNA, and qRT-PCR using SYBR Premix Ex Taq (Takara Bio) and a 7500 RT-PCR system was performed, with 18S ribosomal RNA (rRNA) expression for normalization. The primers used were: 18S rRNA, 5'-AAACGGCTACCACATCCAAG-3' (forward) and 5'-CC-TCCAATGGATCCTCGTTA-3' (reverse); AGAP2-AS1, 5'-TCCTCAAACTGGCTGCCTC-3' (forward) and 5'-GACATCAGGGAGGACGGTCT-3' (reverse).

Cell culture and transfection

Human melanoma cell lines (A375, A875, and MV3) and normal human epidermal melanocytes were purchased from the Cell Biology Department of the Chinese Academy of Sciences (Shanghai, China). Cells were cultured in Dulbecco's Modified Eagle Medium (DMEM) (Gibco Laboratories, Gaithersburg, MD, USA) supplemented with 10% fetal bovine serum (FBS) and incubated at 37°C in 5% CO₂. Lipofectamine 2000 transfection reagent (Invitrogen) was used to transfect A375 and A875 cells with si-AGAP2-AS1, si-*BRD7*, or negative control siRNA (si-NC). The siRNA sequences were: si-AGAP2-AS1#1, 5'-UUGAUCCUGGUCU-UGCAG-3'; si-AGAP2-AS1#2, 5'-AGGUCAAGGU-AAGAGUUUG-3'; si-*BRD7*#1, 5'-AUACGGAUAAU-CUUGGCAC-3'; si-*BRD7*#2, 5'-UAAAUCAUGGCA-UUAGUAC-3'; and si-NC, 5'-UUCUCCGAACGUG-UCACGU-3'. GenePharma (Suzhou, China) synthesized the plasmid vectors (pcDNA3.1-AGAP2-AS1, pcDNA3.1-*BRD7*, pcDNA3.1-MYC, and empty vector); Lipofectamine 2000 was used for transfection. Cell harvest for analysis was performed 48-h post-transfection.

Cell viability and migration

Cell viability was monitored as previously described (Cell Counting Kit 8 (CCK-8);

AGAP2-AS1 promotes skin cutaneous melanoma progression

Beyotime Biotechnology, Beijing, China) [20]. After transfection, the A875 or A375 cells were added to 96-well plates. A Molecular Devices LLC microplate reader (Sunnyvale, CA, USA) was used to obtain optical absorbance (450 nm) values. Cells cultured for two weeks in 10% FBS (six-well plates, 500 cells/well) were used for colony formation assays. Then, the cells were fixed (4% paraformaldehyde) and stained (0.1% crystal violet, Beyotime Biotechnology) as previously described [21].

Twenty-four-well Transwell chambers (Corning Inc., Corning, NY, USA) were used for the migration assays. After a 48-h transfection period, the A875 or A375 cells were resuspended in the upper chamber in 200 μ L serum-free DMEM, with 700 μ L DMEM supplemented with 20% FBS in the lower chamber. After a 48-h incubation, the cells in the upper chamber were removed using a cotton swab. Lower chamber cells were fixed (4% paraformaldehyde) and stained (0.1% crystal violet; Beyotime Biotechnology). Five fields were randomly selected and counted in each well.

In vivo assays

Pathogen-free conditions were used for the four-week-old male athymic BALB/c nude mice included in the study; the mice were treated according to a standard protocol [22]. A375 cells with sh-AGAP2-AS1 (GenePharma) stable transfection or empty vector were injected into the flanks of each mouse (5×10^6 cells, subcutaneous route). Every 3 days, tumor growth was assessed by calculating tumor volume: $V = 0.5 \times D \times d^2$ (V , volume; D , longitudinal diameter; d , latitudinal diameter). The difference between the treatment and control groups was obvious by 15 d. Therefore, all mice were euthanized, and tumors were excised, photographed, and weighed. Tumor cell proliferation was assessed using immunostaining of Ki67. Guide for the Care and Use of Laboratory Animals (US National Institutes of Health) guidelines were strictly followed. The Committee on the Ethics of Animal Experiments, Nanjing Medical University, approved the study protocol.

In vitro transcription, RNA pull-down, and liquid chromatography-tandem mass spectrometry

The Ribo™ RNAmx-T7 Biotin RNA labeling kit (Ribobio, Guangzhou, China) was used for *in vitro* transcription of AGAP2-AS1. After tran-

scription with T7 RNA polymerase, AGAP2-AS1 was labeled with biotin. Then, the Pierce™ Magnetic RNA-protein pull-down kit (Thermo Fisher Scientific, Waltham, MA, USA) was used for RNA pull-down assays. LncRNA-interacting proteins were further detected using mass spectrometric analysis, as previously described [23-25]. Eluted immunocomplexes were resolved using SDS-PAGE (sodium dodecyl sulfate-polyacrylamide gel electrophoresis), followed by western blot.

Western blot

Standard procedures were used for western blot [26, 27]. After separation by 10% SDS-PAGE, protein lysates were transferred to polyvinylidene difluoride membranes (Millipore, Burlington, MA, USA), blocked with Tris-buffered saline containing 5% non-fat milk, and incubated overnight at 4°C with primary antibodies: anti-BRD7 (1:1000 dilution; ProteinTech, Wuhan, China), anti-c-Myc (1:1000 dilution; ProteinTech), and anti-Tubulin (1:10000 dilution; Beyotime). After primary antibody incubation, membranes were washed three times (10 min per wash) in a solution of Tris-buffered saline and polysorbate 20, followed by a 1 h incubation at room temperature with horseradish peroxidase-conjugated secondary antibodies. Blot results were detected using an ECL-PLUS kit (Millipore); tubulin was used as an internal control.

RIP

RNA binding to BRD7 was verified using RIP assays; an anti-BRD7 antibody and Magna RIP™ RNA-binding protein immunoprecipitation kit (Millipore) were used. First, RIP lysis buffer was used to lyse A875 and A375 cells. The cell extract was then incubated with protein A/G beads conjugated with the specific antibodies or control immunoglobulin G (IgG) (4°C, 12 h). To remove proteins, the beads were incubated with proteinase K (0.5 mg/mL) and SDS (0.1%), after using wash buffer. The purified RNA was assessed using qRT-PCR analysis to estimate interactions between BRD7 and AGAP2-AS1.

Co-immunoprecipitation

For co-immunoprecipitation assays, A875 and A375 cells were transfected with si-AGAP2-AS1 or si-NC, respectively. After lysis (cell lysis buf-

AGAP2-AS1 promotes skin cutaneous melanoma progression

fer) and centrifugation (12,000×g, 15 min), the supernatant was incubated with anti-BRD7 antibody (ProteinTech) (4°C, overnight). Subsequently, the immune complexes were isolated and purified according to standard protocols [28, 29]. The co-immunoprecipitation proteins were then eluted and analyzed using western blot and c-Myc antibody (ProteinTech). The input was used as the baseline; IgG was the NC.

Statistical analysis

SPSS version 20.0 software (IBM Corporation, Armonk, NY, USA) was used for all statistical analyses. Student's *t* tests, chi-squared tests, and Mann-Whitney *U* tests were performed to examine between-group differences. Survival curves were estimated using Kaplan-Meier survival analysis, and they were compared using log-rank tests. *P* < 0.05 indicates a significant difference.

Results

AGAP2-AS1 is upregulated in patients with SKCM and is associated with a worse prognosis

To investigate the hypothesis that AGAP2-AS1 had a role in the oncogenesis of SKCM progression, AGAP2-AS1 expression in normal tissues and in SKCM samples was analyzed using TCGA data. AGAP2-AS1 expression in SKCM tissues was markedly upregulated, compared with those in normal tissues (**Figure 1A**), and also increased with T stage development (**Figure 1B**). This result suggested that high AGAP2-AS1 expression was more frequent in patients with advanced-stage SKCM. Kaplan-Meier survival analysis demonstrated that, compared to those with low AGAP2-AS1 expression levels, patients with SKCM with high AGAP2-AS1 expression had markedly shorter OS (**Figure 1C**), disease-specific survival (**Figure 1D**), and PFI (**Figure 1E**) times. AGAP2-AS1 expression was found in samples of SKCM tissues, normal skin cell lines, and SKCM cell lines. A FISH assay of AGAP2-AS1 expression in a tissue microarray with 25 SKCM and paired adjacent normal tissues revealed significant overexpression of AGAP2-AS1 in SKCM tissue samples, compared with samples of adjacent normal tissues (**Figure 1F** and **1G**). In the A375, A875, and MV3 SKCM cell lines, AGAP2-AS1

expression was upregulated compared with that in normal human epidermal melanocytes. AGAP2-AS1 was significantly overexpressed in A375 and A875 cells and was overexpressed to a lesser extent in MV3 cells (**Figure 1H**). Therefore, we selected A375 and A875 (i.e., the two cell lines with higher expression) for further examination.

Silencing AGAP2-AS1 inhibits in vitro and in vivo SKCM tumorigenesis

To investigate the effects of AGAP2-AS1 on SKCM tumorigenesis, the A375 and A875 SKCM cell lines were transfected with si-AGAP2-AS1#1 and si-AGAP2-AS1#2, which resulted in decreased AGAP2-AS1 expression. The results revealed that both siRNAs decreased AGAP2-AS1 expression (**Figure 2A**). The CCK-8 assay results showed that proliferation of cells transfected with AGAP2-AS1 siRNA was markedly decreased (**Figure 2B** and **2C**). We further examined the effect of AGAP2-AS1 inhibition on colony formation and migration of SKCM cells. The results revealed that inhibition of AGAP2-AS1 correlated with significant reductions in colony numbers (**Figure 2D** and **2E**) and fewer migrated cells (**Figure 2F** and **2G**). Taken together, these findings indicated that AGAP2-AS1 silencing inhibited aspects of in vitro SKCM tumorigenesis, including cell proliferation, colony formation, and migration.

We also performed tumor formation experiments in nude mice. Mice were injected (subcutaneous route) with A375 cells with stable sh-AGAP2-AS1 transfection, or with control cells. We found AGAP2-AS1 knockdown decreased tumor growth and weight (**Figure 3A-C**). Immunofluorescence staining revealed that mice injected with sh-AGAP2-AS1-transfected cells had a decrease in Ki67-positive cells (**Figure 3D** and **3E**). This result suggested that cell proliferation in vivo was inhibited by AGAP2-AS1 knockdown.

AGAP2-AS1 interacts with BRD7 in SKCM cells

To examine the non-coding function of AGAP2-AS1 in SKCM progression, RNA pull-down assays, followed by proteomic analysis of the AGAP2-AS1-associated protein complex in A375 cells, were performed (**Figure 4A**). We identified 34 proteins from three independent

AGAP2-AS1 promotes skin cutaneous melanoma progression

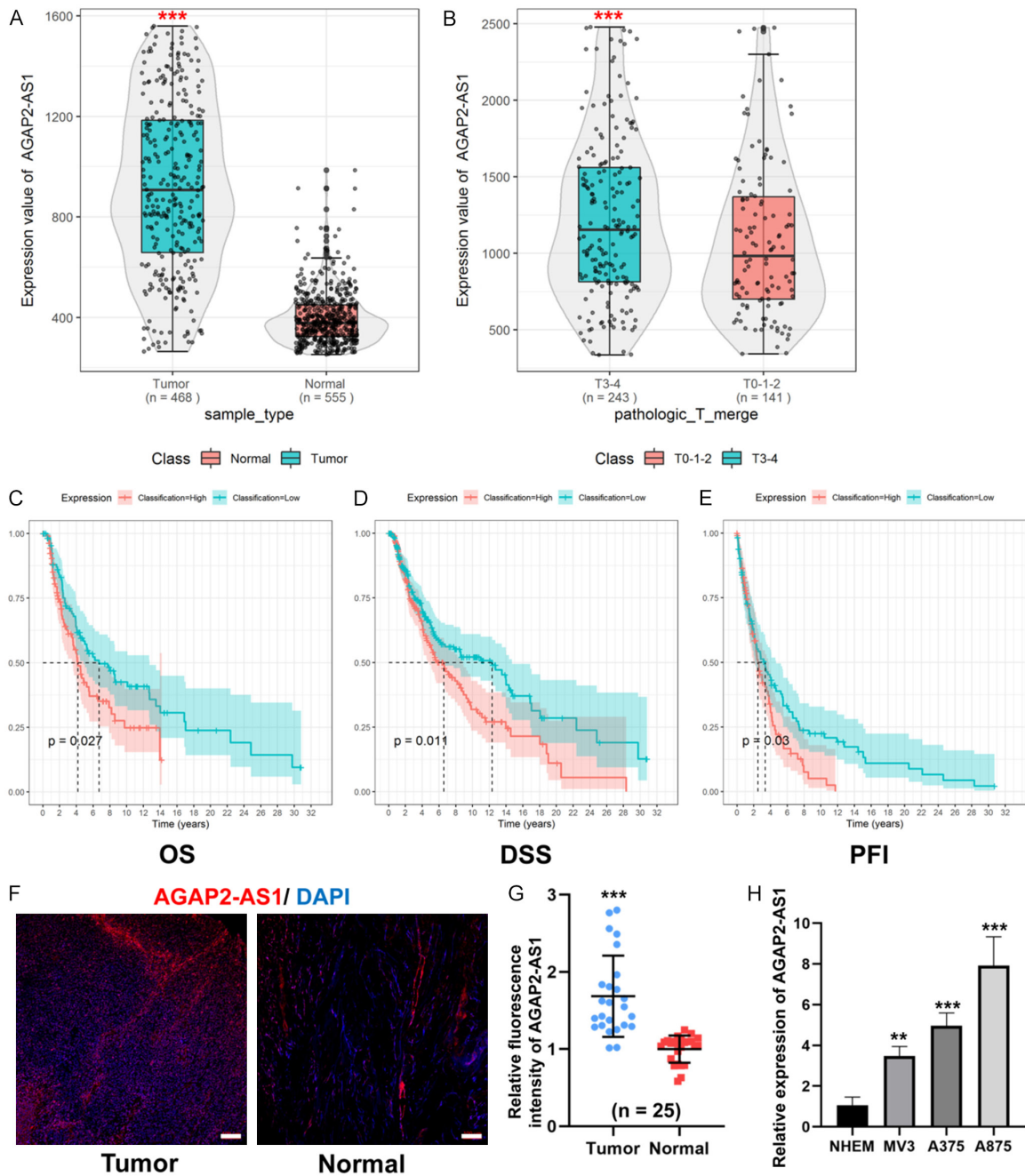


Figure 1. AGAP2 Antisense RNA 1 (AGAP2-AS1) is upregulated in patients with skin cutaneous melanoma (SKCM) tissues and cells and is associated with a worse prognosis. (A) AGAP2-AS1 expression level in SKCM tissues was markedly upregulated, compared with that in normal counterparts. (B) Expression of AGAP2-AS1 remarkably increased with T stage development. (C-E) Patients with SKCM with high AGAP2-AS1 expression had markedly shorter overall survival (OS), disease-specific survival, and PFI. (F) Fluorescence in situ hybridization (FISH) assay of AGAP2-AS1 expression in SKCM tissues and adjacent normal tissues. Scale bar: 100 μ m. (G) Quantification of (F). (H) Quantitative real-time polymerase chain reaction (qRT-PCR) of AGAP2-AS1 expression in SKCM cell lines (A375, A875, and MV3) and normal human epidermal melanocytes (NHEM). n = 3 for each group. ** $P < 0.01$, *** $P < 0.001$.

experiments (Figure 4B and Table S1). Among these proteins, other studies found that BRD7 has a crucial tumor-regulating function in numerous malignancies [30, 31]. Subsequently,

western blot and RIP assay results confirmed the AGAP2-AS1 and BRD7 interaction in extracts from A875 and A375 cells (Figure 4C-E).

AGAP2-AS1 promotes skin cutaneous melanoma progression

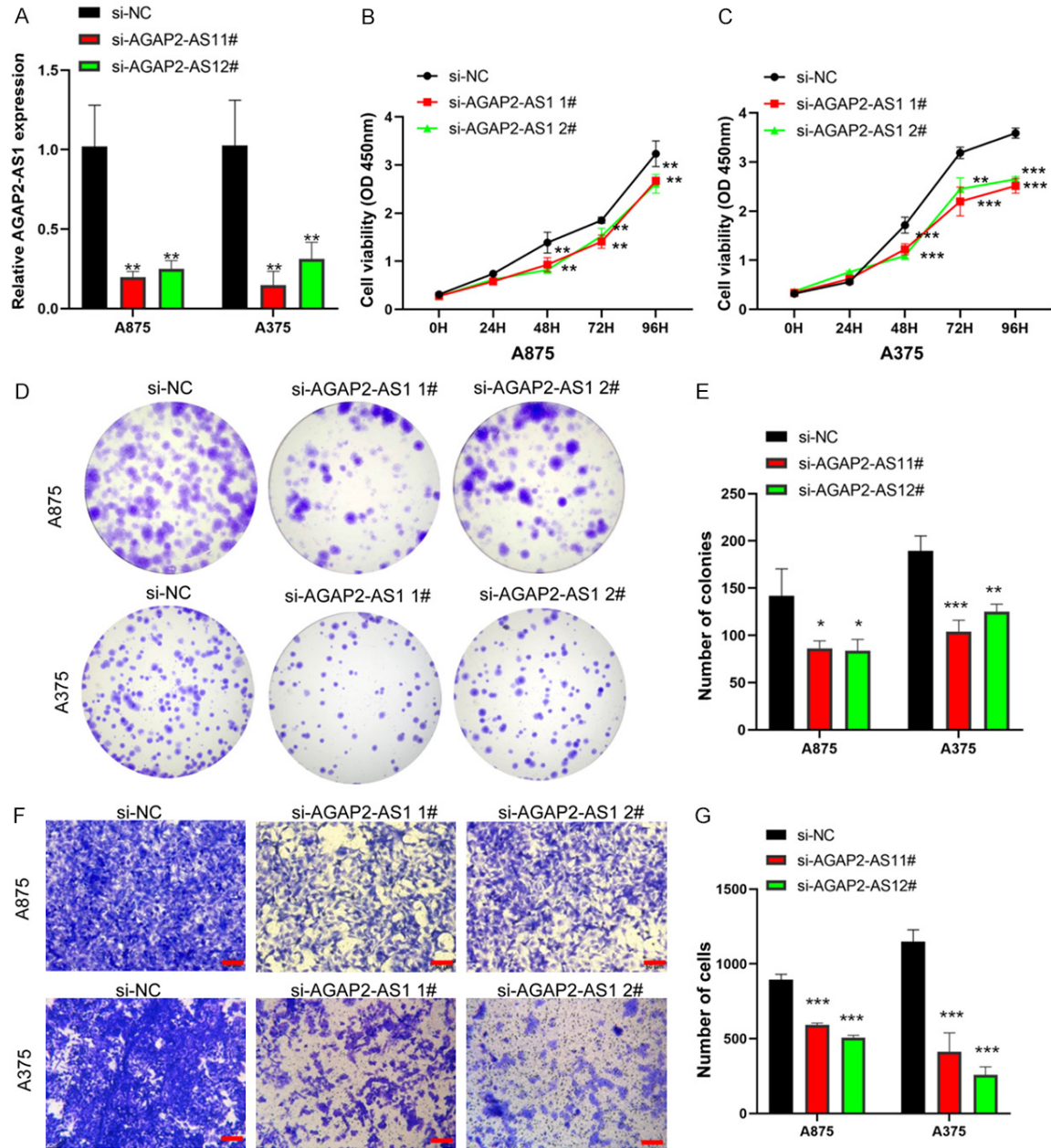


Figure 2. AGAP2 Antisense RNA 1 (AGAP2-AS1) knockdown reduces the malignant level of skin cutaneous melanoma (SKCM) cells in vitro. A. A875 and A375 SKCM cell lines were transfected with si-AGAP2-AS1#1 and si-AGAP2-AS1#2, which led to decreased AGAP2-AS1 expression. $n = 3$ for each group. B, C. Cell Counting Kit 8 (CCK-8) assays revealed cell proliferation decreased after downregulation of AGAP2-AS1. $n = 4$ for each group. D, E. Cell colony numbers decreased after downregulation of AGAP2-AS1. $n = 3$ for each group. F, G. Transwell assays revealed that cell migration decreased after downregulation of AGAP2-AS1. $n = 3$ for each group. Scale bar: 50 μ m. * $P < 0.05$, ** $P < 0.01$, *** $P < 0.001$.

Knockdown of BRD7 suppresses proliferation and migration in SKCM cells

To determine the role of *BRD7* in SKCM cells, si-*BRD7*#1, si-*BRD7*#2, and si-NC were transfected into A875 and A375 cells to knock down *BRD7* expression, followed by CCK-8 and colo-

ny formation assays. In both cell lines, knockdown of *BRD7* expression resulted in cell growth inhibition (Figure 5A-E). Transwell assay results indicated that compared with control cell migration, SKCM cell migration was inhibited by *BRD7* knockdown (Figure 5F and 5G). These results suggest that knockdown of *BRD7*

AGAP2-AS1 promotes skin cutaneous melanoma progression

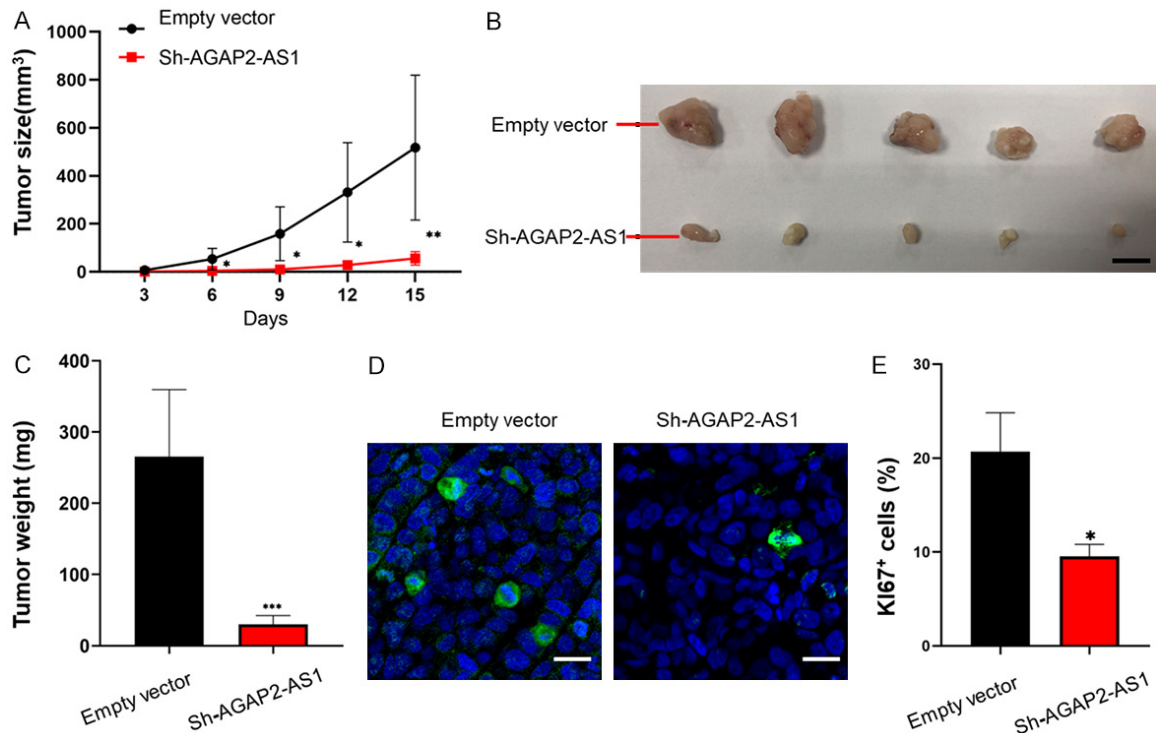


Figure 3. Silencing of AGAP2 Antisense RNA 1 (AGAP2-AS1) inhibits skin cutaneous melanoma (SKCM) tumorigenesis in vivo. A, B. Knockdown of AGAP2-AS1 could decrease tumor growth. $n = 5$ for each group. Scale bar: 1 cm. C. Knockdown of AGAP2-AS1 could decrease tumor weights. $n = 5$ for each group. D, E. Mice injected with sh-AGAP2-AS1-transfected cells had a decrease in Ki67-positive cells, suggesting that AGAP2-AS1 knockdown inhibited cell proliferation in vivo. $n = 5$ for each group. Scale bar: 20 μm . * $P < 0.05$, ** $P < 0.01$, *** $P < 0.001$.

expression is tumor-suppressive and impedes SKCM cell proliferation and migration phenotypes.

c-Myc is a downstream target of the AGAP2-AS1/BRD7 axis

Zhao *et al.* [31] found that BRD7 stabilizing c-Myc promotes colorectal cancer cell proliferation and tumor growth. We, therefore, hypothesized that c-Myc was the potential downstream target protein of the AGAP2-AS1/BRD7 axis in SKCM cells. Western blot results indicated that when AGAP2-AS1 or BRD7 was knocked down, c-Myc protein levels were significantly reduced (Figure 6A and 6B); but, overexpression of AGAP2-AS1 or BRD7 significantly accelerated c-Myc protein levels (Figure 6C and 6D). AGAP2-AS1 knockdown in SKCM cells did not alter the levels of expression of BRD7 (Figure 6E and 6F). Nevertheless, co-immunoprecipitation experiments found that knockdown of AGAP2-AS1 attenuated the interaction between BRD7 and c-Myc (Figure 6G). This result further supported the hypothesis that AGAP2-AS1 was

required for BRD7-mediated stabilization of c-Myc.

c-Myc regulation is involved in oncogenic function of AGAP2-AS1

To investigate whether knockdown of AGAP2-AS1 or BRD7 inhibited SKCM malignancy through c-Myc, we performed a rescue experiment to observe the changes in A875 and A375 cell growth and migration. We co-transfected pcDNA3.1-MYC with si-AGAP2-AS1 or si-BRD7. CCK-8 and colony formation assay results indicated that knockdown of AGAP2-AS1 or BRD7 decreased A875 and A375 cell growth, and co-transfection of pcDNA3.1-MYC largely restored SKCM cell proliferation (Figure 7A-D) and migration (Figure 7E and 7F).

Discussion

SKCM is the most aggressive skin malignancy that has a high mortality rate due to high rates of metastasis and recurrence. The anti-programmed cell death protein 1 and anti-CTLA-4

AGAP2-AS1 promotes skin cutaneous melanoma progression

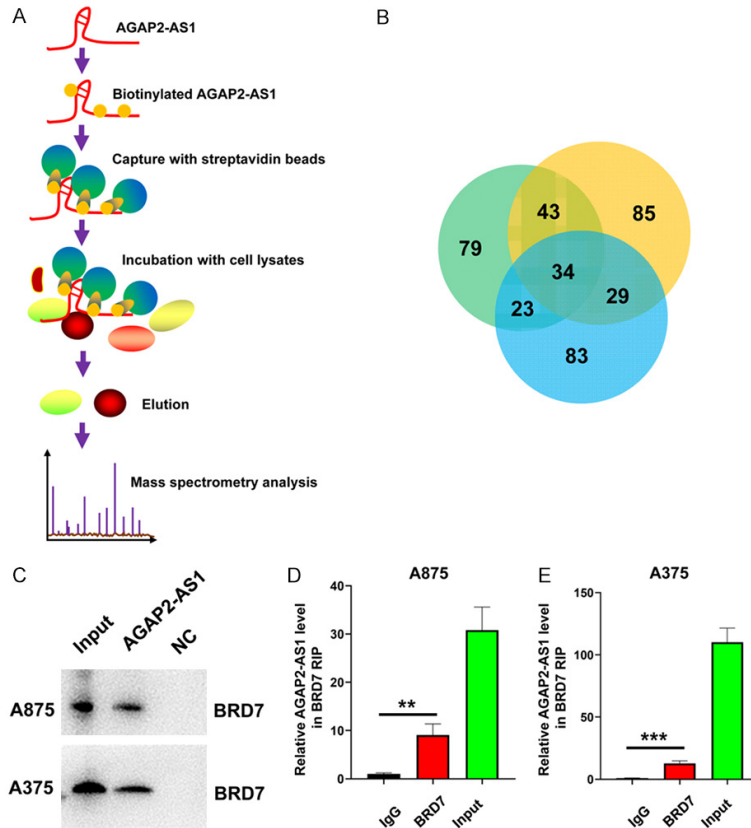


Figure 4. AGAP2 Antisense RNA 1 (AGAP2-AS1) interacts with bromodomain containing 7 (BRD7) in skin cutaneous melanoma (SKCM) cells. **A.** Flowchart of RNA pull-down and mass spectrometry assays. **B.** Venn diagrams of proteins identified using mass spectrometry, from three independent RNA pull-down assays. **C.** Biotinylated AGAP2-AS1 RNAs were incubated with A875 and A375 cell lysates, respectively. RNA-protein complexes were examined using western blot analysis with anti-BRD7 antibody. The antisense strand of AGAP2-AS1 was used as the negative control (NC). **D, E.** RIP experiments of AGAP2-AS1 binding to BRD7 in A875 and A375 cell lysates. $n = 3$ for each group. Rabbit IgG was included as the NC for the immunoprecipitation.

antibodies used in BRAF/MEK targeted- and immunotherapies benefit only 30%-40% of patients with SKCM [2]. Identification of novel SKCM molecular markers and new effective therapeutic strategies may improve disease outcomes. AGAP2-AS1 has a crucial role in the tumorigenesis and progression of multiple cancers. However, our understanding of the effects and mechanisms of AGAP2-AS1 in SKCM progression is incomplete. Previous studies have shown that AGAP2-AS1 is widely dysregulated and associated with tumorigenesis in multiple malignancies [13, 32, 33]. AGAP2-AS1 is an important oncogenic factor. Upregulation is associated with a worse prognosis for patients with SKCM. Knockdown of AGAP2-AS1 increases erastin-mediated iron

death in SKCM cells [33]. In this study, AGAP2-AS1 was upregulated in human SKCM tissues and cells and predicted a worse prognosis. Compared with control group cells, AGAP2-AS1 knockdown in SKCM cells resulted in a significant decrease in cell proliferation and migration. Knockdown of AGAP2-AS1 in SKCM cells resulted in suppressed SKCM tumor growth in a xenograft tumor model. To our knowledge, this was the first systematic study with findings that suggested AGAP2-AS1 was a crucial regulator of SKCM tumorigenesis.

An important mechanism of lncRNAs is the scaffolding of protein-protein interactions. We used RNA pull-down and RIP assays to elucidate molecular mechanisms of AGAP2-AS1 in SKCM. AGAP2-AS1 directly interacted with BRD7 to regulate SKCM tumorigenesis. BRD7 is an important transcriptional regulatory factor. It participates in cell-based processes including cell cycle progression, transcriptional regulation, and chromatin remodeling. It also has significant roles in the

pathogenesis of multiple cancers [34]. *BRD7* is overexpressed in SKCM tissue samples and is associated with poor outcomes [3]. After knocking down *BRD7*, SKCM cell proliferation, colony formation, and migration were significantly decreased in the *BRD7*-silenced group when compared with the normal group. Taken together, these results suggest that AGAP2-AS1 synergistically cooperates with BRD7 to regulate SKCM progression.

C-Myc is involved in 15% of the transcriptome genes. It regulates the cell cycle, cell proliferation and differentiation, metabolism, and apoptosis [35, 36]. Because c-Myc is widely dysregulated and associated with tumorigenesis in multiple malignancies, it has appeal as a thera-

AGAP2-AS1 promotes skin cutaneous melanoma progression

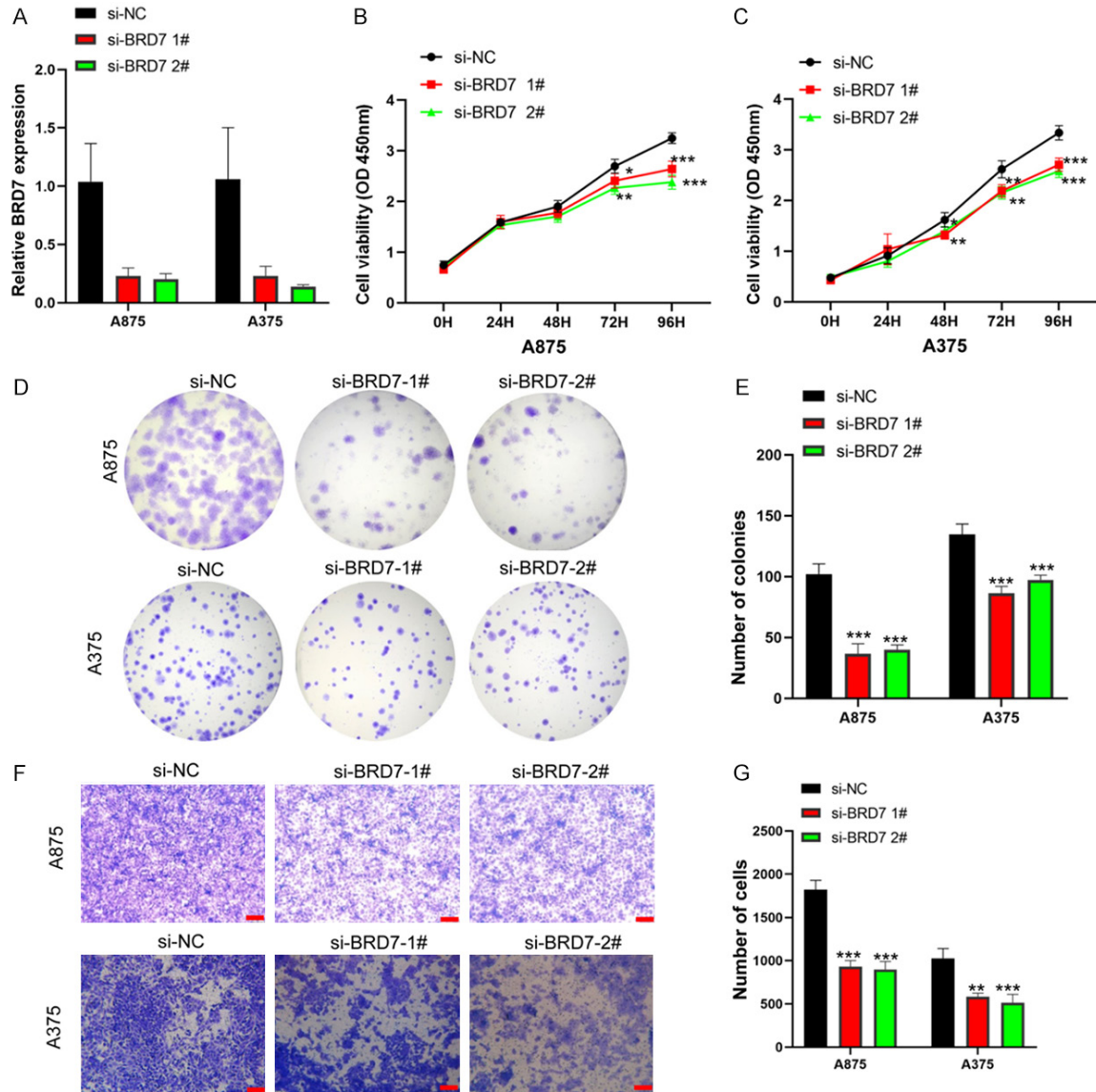
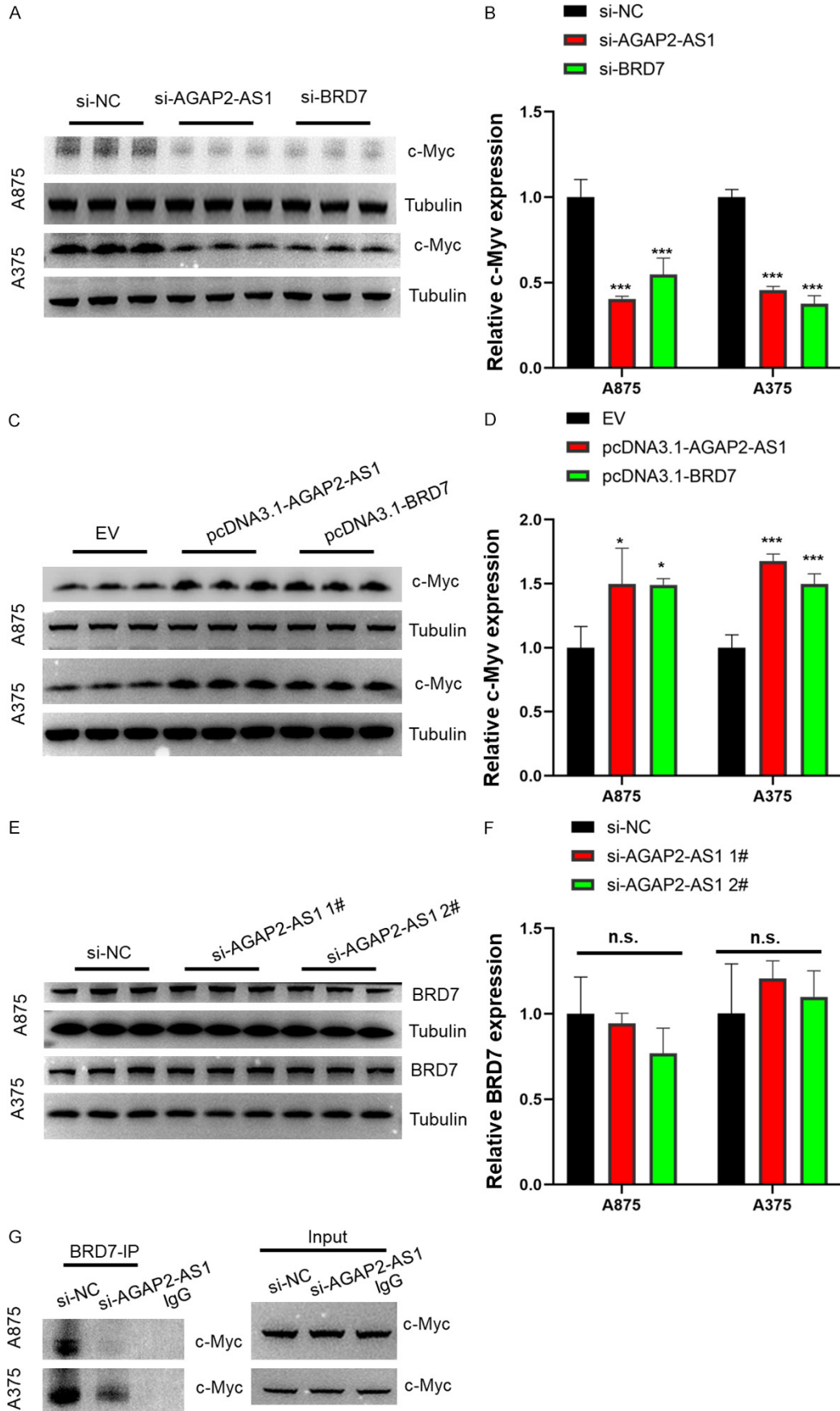


Figure 5. Bromodomain containing 7 (*BRD7*) knockdown suppressed proliferation and migration of skin cutaneous melanoma (SKCM) cells. A. A875 and A375 cells transfected with si-NC (negative control) or si-*BRD7*#1 and si-*BRD7*#2 were subjected to quantitative real-time polymerase chain reaction (qRT-PCR) for *BRD7* expression. $n = 3$ for each group. B, C. Cell Counting Kit 8 (CCK-8) assay of proliferation ability in transfected cells. $n = 4$ for each group. D, E. Colony formation assay of cloning ability in transfected cells. $n = 3$ for each group. F, G. Transwell assay of migration in transfected cells. $n = 3$ for each group. Scale bar: 100 μm . * $P < 0.05$, ** $P < 0.01$, *** $P < 0.001$.

peutic target. However, due to the inherent disordered nature of its protein structure, c-Myc has been generally considered “undruggable” [36]. *BRD7* silencing leads to significantly decreased c-Myc expression and a reduction in the c-Myc protein half-life. This result suggests that *BRD7* can be used to overcome c-Myc’s “undruggable” nature [31]. In this study, we further examined whether AGAP2-AS1 affected SKCM tumorigenesis through the *BRD7*/c-Myc signaling pathway. AGAP2-AS1

and *BRD7* knockdown resulted in decreased expression of c-Myc; AGAP2-AS1 and *BRD7* overexpression led to increased c-Myc levels. Co-immunoprecipitation experiments found that AGAP2-AS1 knockdown affected the binding of c-Myc to *BRD7*. This result suggested that AGAP2-AS1 was the key molecule required for effective *BRD7* regulation of c-Myc stability. These findings provide a new understanding of the relationship between AGAP2-AS1 and *BRD7* during SKCM progression.

AGAP2-AS1 promotes skin cutaneous melanoma progression



AGAP2-AS1 promotes skin cutaneous melanoma progression

Figure 6. C-Myc is a potential downstream target of the AGAP2-AS1/BRD7 axis. A-D. Western blot analysis of c-Myc after AGAP2 Antisense RNA 1 (AGAP2-AS1) or bromodomain containing 7 (*BRD7*) downregulation or overexpression in A875 and A375 cells. Tubulin was used as an internal control. n = 3 for each group. E, F. Western blot analysis of BRD7 after AGAP2-AS1 downregulation in A875 and A375 cells. n = 3 for each group. G. Co-immunoprecipitation assay of interaction between BRD7 and c-Myc in A875 and A375 cells transfected with si-AGAP2-AS1 or si-NC (negative control). * $P < 0.05$, *** $P < 0.001$; n.s., not significant.

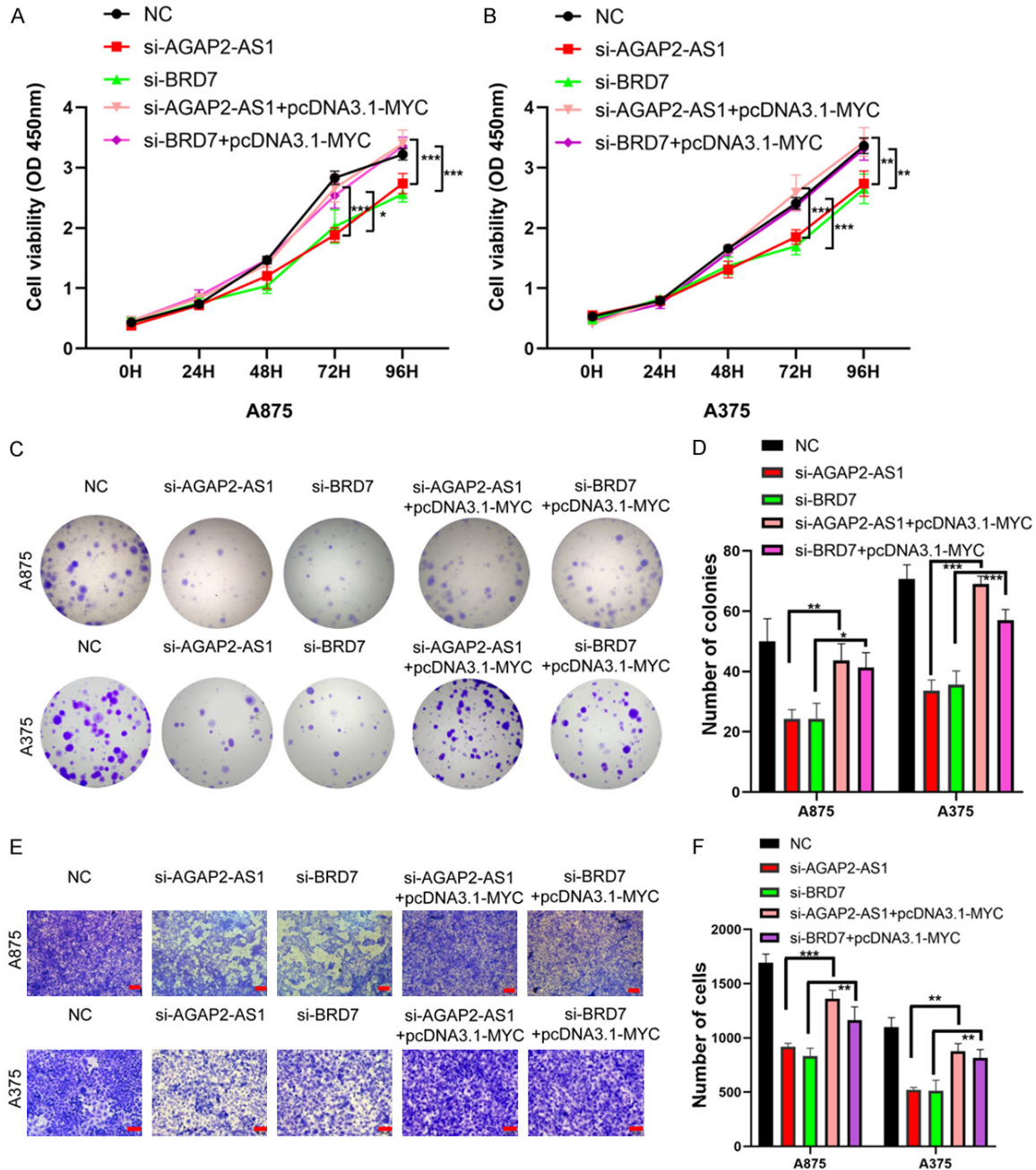


Figure 7. Regulation of c-Myc is involved in the oncogene function of AGAP2 Antisense RNA 1 (AGAP2-AS1). (A, B) Cell Counting Kit 8 (CCK-8) and (C, D) colony formation assays to determine cell viability of A875 and A375 cells co-transfected with pcDNA3.1-MYC and si-AGAP2-AS1 or si-*BRD7*. (E, F) Transwell assays to investigate changes in migratory abilities of A875 and A375 cells co-transfected with pcDNA3.1-MYC and si-AGAP2-AS1 or si-*BRD7*. Scale bar: 100 μm . * $P < 0.05$, ** $P < 0.01$, *** $P < 0.001$.

Conclusions

In summary, this study was the first to find that for patients with SKCM, AGAP2-AS1 upregulation was significantly associated with a worse prognosis. AGAP2-AS1 promoted SKCM cell proliferation, colony formation, and migration in vitro and in vivo, and AGAP2-AS1 participated in the oncogenesis of SKCM, at least in part via the BRD7/c-Myc signaling pathway.

Acknowledgements

A grant from the Suzhou Key Clinical Diseases Funding program (LCZX202109) supported this study.

Disclosure of conflict of interest

None.

Address correspondence to: Qihong Qian, Department of Dermatology, First Affiliated Hospital of Soochow University, Suzhou 215006, Jiangsu, China. Tel: +86-17712661289; E-mail: qianqihong@suda.edu.cn

References

[1] Yang RH, Liang B, Li JH, Pi XB, Yu K, Xiang SJ, Gu N, Chen XD and Zhou ST. Identification of a novel tumour microenvironment-based prognostic biomarker in skin cutaneous melanoma. *J Cell Mol Med* 2021; 25: 10990-11001.

[2] Rebecca VW, Somasundaram R and Herlyn M. Pre-clinical modeling of cutaneous melanoma. *Nat Commun* 2020; 11: 2858.

[3] Mason LD, Chava S, Reddi KK and Gupta R. The BRD9/7 inhibitor TP-472 blocks melanoma tumor growth by suppressing ECM-mediated oncogenic signaling and inducing apoptosis. *Cancers (Basel)* 2021; 13: 5516.

[4] Hayward NK, Wilmott JS, Waddell N, Johanson PA, Field MA, Nones K, Patch AM, Kakavand H, Alexandrov LB, Burke H, Jakrot V, Kazakoff S, Holmes O, Leonard C, Sabarinathan R, Mularoni L, Wood S, Xu Q, Waddell N, Tembe V, Pupo GM, De Paoli-Iseppi R, Vilain RE, Shang P, Lau LMS, Dagg RA, Schramm SJ, Pritchard A, Dutton-Regester K, Newell F, Fitzgerald A, Shang CA, Grimmond SM, Pickett HA, Yang JY, Stretch JR, Behren A, Kefford RF, Hersey P, Long GV, Cebon J, Shackleton M, Spillane AJ, Saw RPM, López-Bigas N, Pearson JV, Thompson JF, Scolyer RA and Mann GJ. Whole-genome landscapes of major melanoma subtypes. *Nature* 2017; 545: 175-180.

[5] Wang J, Zhao Y, Tang Y, Li F and Chen X. The role of lncRNA-MEG/miR-21-5p/PDCD4 axis

in spinal cord injury. *Am J Transl Res* 2021; 13: 646-658.

[6] Chen N, Zhu X, Zhu Y, Shi J, Zhang J, Tang C and Chen J. The regulatory relationship and function of lncRNA FAM225A-miR-206-AD-AM12 in gastric cancer. *Am J Transl Res* 2021; 13: 8632-8652.

[7] Perez CAG, Adachi S, Nong QD, Adhitama N, Matsuura T, Natsume T, Wada T, Kato Y and Watanabe H. Sense-overlapping lncRNA as a decoy of translational repressor protein for dimorphic gene expression. *PLoS Genet* 2021; 17: e1009683.

[8] Xing Z, Lin A, Li C, Liang K, Wang S, Liu Y, Park PK, Qin L, Wei Y, Hawke DH, Hung MC, Lin C and Yang L. lncRNA directs cooperative epigenetic regulation downstream of chemokine signals. *Cell* 2014; 159: 1110-1125.

[9] Winkle M, El-Daly SM, Fabbri M and Calin GA. Noncoding RNA therapeutics - challenges and potential solutions. *Nat Rev Drug Discov* 2021; 20: 629-651.

[10] Liu SJ, Dang HX, Lim DA, Feng FY and Maher CA. Long noncoding RNAs in cancer metastasis. *Nat Rev Cancer* 2021; 21: 446-460.

[11] Bao Z, Zheng Q and Li L. Oncogenic roles and mechanisms of lncRNA AGAP2-AS1 in human solid tumors. *Am J Transl Res* 2021; 13: 757-769.

[12] Qi F, Liu X, Wu H, Yu X, Wei C, Huang X, Ji G, Nie F and Wang K. Long noncoding AGAP2-AS1 is activated by SP1 and promotes cell proliferation and invasion in gastric cancer. *J Hematol Oncol* 2017; 10: 48.

[13] Luo W, Li X, Song Z, Zhu X and Zhao S. Long non-coding RNA AGAP2-AS1 exerts oncogenic properties in glioblastoma by epigenetically silencing TFPI2 through EZH2 and LSD1. *Aging (Albany NY)* 2019; 11: 3811-3823.

[14] Shen S, Li K, Liu Y, Liu X, Liu B, Ba Y and Xing W. Silencing lncRNA AGAP2-AS1 upregulates miR-195-5p to repress migration and invasion of EC cells via the decrease of FOSL1 expression. *Mol Ther Nucleic Acids* 2020; 20: 331-344.

[15] Hong S, Yan Z, Song Y, Bi M and Li S. lncRNA AGAP2-AS1 augments cell viability and mobility, and confers gemcitabine resistance by inhibiting miR-497 in colorectal cancer. *Aging (Albany NY)* 2020; 12: 5183-5194.

[16] Mohebi M, Ghafouri-Fard S, Modarressi MH, Dashti S, Zekri A, Kholghi-Oskooei V and Taheri M. Expression analysis of vimentin and the related lncRNA network in breast cancer. *Exp Mol Pathol* 2020; 115: 104439.

[17] Poulet C, Njock MS, Moermans C, Louis E, Louis R, Malaise M and Guiot J. Exosomal long non-coding RNAs in lung diseases. *Int J Mol Sci* 2020; 21: 3580.

[18] Li H, Guo S, Zhang M, Li L, Wang F and Song B. Long non-coding RNA AGAP2-AS1 accelerates

AGAP2-AS1 promotes skin cutaneous melanoma progression

- cell proliferation, migration, invasion and the EMT process in colorectal cancer via regulating the miR-4,668-3p/SRSF1 axis. *J Gene Med* 2020; 22: e3250.
- [19] Li W, Sun M, Zang C, Ma P, He J, Zhang M, Huang Z, Ding Y and Shu Y. Upregulated long non-coding RNA AGAP2-AS1 represses LATS2 and KLF2 expression through interacting with EZH2 and LSD1 in non-small-cell lung cancer cells. *Cell Death Dis* 2016; 7: e2225.
- [20] Yu J, Shen C, Lin M, Chen X, Dai X, Li Z, Wu Y, Fu Y, Lv J, Huang X, Zheng B and Sun F. BMI1 promotes spermatogonial stem cell maintenance by epigenetically repressing Wnt10b/ β -catenin signaling. *Int J Biol Sci* 2022; 18: 2807-2820.
- [21] Zheng B, Liu J, Shi X, Xu J, Zhang K, Zhou H, Wu T, Huang X, Shen C, Liang Y, Zhao D and Guo Y. BMI1 governs the maintenance of mouse GC-2 cells through epigenetic repression of Foxl1 transcription. *Am J Transl Res* 2022; 14: 3407-3418.
- [22] Wang Q, Wu Y, Lin M, Wang G, Liu J, Xie M, Zheng B, Shen C and Shen J. BMI1 promotes osteosarcoma proliferation and metastasis by repressing the transcription of SIK1. *Cancer Cell Int* 2022; 22: 136.
- [23] Liu Y, Yu X, Huang A, Zhang X, Wang Y, Geng W, Xu R, Li S, He H, Zheng B, Chen G and Xu Y. INTS7-ABCD3 interaction stimulates the proliferation and osteoblastic differentiation of mouse bone marrow mesenchymal stem cells by suppressing oxidative stress. *Front Physiol* 2021; 12: 758607.
- [24] Zhang K, Xu J, Ding Y, Shen C, Lin M, Dai X, Zhou H, Huang X, Xue B and Zheng B. BMI1 promotes spermatogonia proliferation through epigenetic repression of Ptprm. *Biochem Biophys Res Commun* 2021; 583: 169-177.
- [25] Zhou J, Li J, Qian C, Qiu F, Shen Q, Tong R, Yang Q, Xu J, Zheng B, Lv J and Hou J. LINC00624/TEX10/NF- κ B axis promotes proliferation and migration of human prostate cancer cells. *Biochem Biophys Res Commun* 2022; 601: 1-8.
- [26] Zheng B, Zhao D, Zhang P, Shen C, Guo Y, Zhou T, Guo X, Zhou Z and Sha J. Quantitative proteomics reveals the essential roles of stromal interaction molecule 1 (STIM1) in the testicular cord formation in mouse testis. *Mol Cell Proteomics* 2015; 14: 2682-2691.
- [27] Yu J, Wu Y, Li H, Zhou H, Shen C, Gao T, Lin M, Dai X, Ou J, Liu M, Huang X, Zheng B and Sun F. BMI1 drives steroidogenesis through epigenetically repressing the p38 MAPK pathway. *Front Cell Dev Biol* 2021; 9: 665089.
- [28] Zhou H, Shen C, Guo Y, Huang X, Zheng B and Wu Y. The plasminogen receptor directs maintenance of spermatogonial stem cells by targeting BMI1. *Mol Biol Rep* 2022; 49: 4469-4478.
- [29] Wu Y, Shen C, Wu T, Huang X, Li H and Zheng B. Syntaxin binding protein 2 in sertoli cells regulates spermatogonial stem cell maintenance through directly interacting with connexin 43 in the testes of neonatal mice. *Mol Biol Rep* 2022; 49: 7557-7566.
- [30] Yu X, Li Z and Shen J. BRD7: a novel tumor suppressor gene in different cancers. *Am J Transl Res* 2016; 8: 742-748.
- [31] Zhao R, Liu Y, Wu C, Li M, Wei Y, Niu W, Yang J, Fan S, Xie Y, Li H, Wang W, Zeng Z, Xiong W, Li X, Li G and Zhou M. BRD7 promotes cell proliferation and tumor growth through stabilization of c-Myc in colorectal cancer. *Front Cell Dev Biol* 2021; 9: 659392.
- [32] Wang W, Yang F, Zhang L, Chen J, Zhao Z, Wang H, Wu F, Liang T, Yan X, Li J, Lan Q, Wang J and Zhao J. LncRNA profile study reveals four-lncRNA signature associated with the prognosis of patients with anaplastic gliomas. *Oncotarget* 2016; 7: 77225-77236.
- [33] An L, Huang J, Ge S, Zhang X and Wang J. LncRNA AGAP2-AS1 facilitates tumorigenesis and ferroptosis resistance through SLC7A11 by IGF2BP2 pathway in melanoma. *Comput Math Methods Med* 2022; 2022: 1972516.
- [34] Park SW and Lee JM. Emerging roles of BRD7 in pathophysiology. *Int J Mol Sci* 2020; 21: 7127.
- [35] Kress TR, Sabò A and Amati B. MYC: connecting selective transcriptional control to global RNA production. *Nat Rev Cancer* 2015; 15: 593-607.
- [36] Llombart V and Mansour MR. Therapeutic targeting of “undruggable” MYC. *EBioMedicine* 2022; 75: 103756.

AGAP2-AS1 promotes skin cutaneous melanoma progression

Table S1. Putative interactors identified from three independent RNA pull-down assays in this study

Gene names	iBAQ AGAP2- AS1_rep1	iBAQ AGAP2- AS1_rep2	iBAQ AGAP2- AS1_rep3	iBAQ Control_ rep1	iBAQ Control_ rep2	iBAQ Control_ rep3
ABR	363240	518090	373600	0	0	0
AFG3L2	142730	82143	97608	0	0	0
ANKHD1	112370	54941	87373	0	0	0
AP2A2	848400	98910	126020	0	0	0
ARID1A	422480	114700	255790	0	0	0
ATP5H	1928100	1590600	847480	0	0	0
ATP6V1H	661760	131880	195740	0	0	0
BPIFA1	10969000	9710500	10782000	0	0	0
BPIFB1	938500	1594000	2484600	0	0	0
BRD7	794600	183060	316180	0	0	0
C1orf131	2023700	1791000	1535700	0	0	0
DDX19A	144130	126040	335450	0	0	0
DSG1	816040	994800	438830	0	0	0
EIF4E	695380	848350	459510	0	0	0
EXOC2	216010	326450	226660	0	0	0
EXOC4	742280	236910	383170	0	0	0
GNAS	1643800	1777600	1866900	0	0	0
LIMS1	1482000	2197900	1520100	0	0	0
LSG1	663270	839250	1035700	0	0	0
MED11	2548200	2374700	2664200	0	0	0
MED15	453510	106590	262850	0	0	0
MED20	4460500	6362800	9287500	0	0	0
MED21	4563700	2730600	3442800	0	0	0
MED23	76481	418960	343350	0	0	0
MED6	401800	486160	246010	0	0	0
MTAP	1516300	1430200	2473800	0	0	0
NUP62	2824700	3378900	2000900	0	0	0
PIGR	1364100	218920	1054300	0	0	0
PSMC6	177020	110280	203030	0	0	0
PTPN13	214730	25789	181840	0	0	0
S100A8	6275500	4110900	3357600	0	0	0
SPICE1	121720	161130	724700	0	0	0
SYT1	446190	2894100	947320	0	0	0
TRIP13	346060	996380	292260	0	0	0